

Petrography and geochemical analysis of Arctic ikaite pseudomorphs from Utqiagvik (Barrow), Alaska

Bo P. Schultz¹, Jennifer M. Huggett^{2,3}, George L. Kennedy^{4,5}, Paul Burger⁶, Henrik Friis⁷, Anne M. Jensen⁸, Marie Kanstrup⁹, Stefano M. Bernasconi¹⁰, Nicolas Thibault¹¹, Clemens V. Ullmann¹², and Madeleine L. Vickers¹³

¹ Fur Museum, Museum Salling, Nederby 28, 7884 Fur, Denmark

² Petroclays, Oast House, Sandy Cross Lane, Heathfield, Sussex TN21 8QP, UK

³ The Natural History Museum, Cromwell road, London SW7 5BD, UK

⁴ San Diego Paleontological Associates, 8997 Moisan Way, La Mesa, California 91941, USA

⁵ Natural History Museum of Los Angeles County, Los Angeles, California 90007, USA

⁶ National Park Service-Alaska, Alaska, USA

⁷ Department of Geoscience, Århus University, Århus C, Denmark

⁸ Department of Anthropology, University of Alaska, Fairbanks, Alaska, USA

⁹ Århus AMS Centre, Århus University, Ny Munkegade 120, DK-8000 Århus C, Denmark

¹⁰ Geologisches Institut, Departement Erdwissenschaften, ETH Zürich, Sonneggstrasse 5, 8092 Zürich, Switzerland

¹¹ IGN, University of Copenhagen, Øster Voldgade 10, DK-1350 Copenhagen, Denmark

¹² Camborne School of Mines, University of Exeter, Penryn Campus, Penryn, Cornwall TR10 9FE, U.K

¹³ CEED University of Oslo, P.O. Box 1028, Blindern, 0315 Oslo, Norway

E-mail corresponding author (Bo P. Schultz) bosc@museumsalling.dk

Keywords:

- Holocene
- Coastal
- Ikaite
- Glendonite
- Petrology
- Isotopes

Electronic Supplement 1:
[Data_Barrow_supplementary](#)

Received:
19. August 2022

Accepted:
5. December 2022

Published online:
30. January 2023

Ikaite and pseudomorphs thereafter (“glendonites”) are a potentially powerful tool for palaeoclimatic studies, as a low-temperature proxy. However, much uncertainty still surrounds the drivers of ikaite formation, in particular prerequisite thermal and chemical conditions. Furthermore, the ikaite to glendonite transformation is not fully understood, and it was unclear which calcite phases in glendonites were ikaite-derived and which were later diagenetic calcites. This leads to difficulties in choosing which phase to analyse in order to reconstruct the original ikaite growth environmental conditions. Petrographic examination of air-transformed ikaite from the Isatkoak Lagoon in Utqiagvik, Alaska, confirms that both ‘Type I’ and ‘Type II’ calcite phases seen in glendonites are directly derived from ikaite breakdown and not from secondary sources. Clumped isotope temperature reconstructions for transformed ikaites from Utqiagvik, and comparison to Recent glendonites from the White Sea, Russia, confirm that clumped isotope thermometry may be used to reconstruct ikaite growth temperatures, whilst stable isotopes and minor elemental analysis reveal that a range of geochemical conditions characterise ikaite growth sites.

Schultz, B.P., Huggett, J.M., Kennedy, G.L., Burger, P., Friis, H., Jensen, A.M., Kanstrup, M., Bernasconi, S.M., Thibault, N., Ullmann, C.V. & Vickers, M.L. 2022: Petrography and geochemical analysis of Arctic ikaite pseudomorphs from Utqiagvik (Barrow), Alaska. *Norwegian Journal of Geology* 103, 202303.
<https://dx.doi.org/10.17850/njg103-1-3>

© Copyright the authors.

This work is licensed under a Creative Commons Attribution 4.0 International License.

Introduction

Ikaite, metastable calcium carbonate hexahydrate ($\text{CaCO}_3 \cdot 6\text{H}_2\text{O}$), and pseudomorphs thereafter (known as 'glendonites'), have been of interest to the palaeoclimate community as a potential cold climate indicator since the 1980s (e.g., Kemper, 1987; Rogov et al., 2021 and references therein). Yet much debate surrounds the use of glendonites for this purpose, due to recent laboratory experiments synthesising ikaite at warm temperatures ($>12^\circ\text{C}$; Purgstaller et al., 2017; Stockmann et al., 2018; Tollefsen et al., 2020), and uncertainties surrounding the nature of the ikaite to glendonite transformation process (e.g., Tollefsen et al., 2020; Vickers et al., 2022). Ikaite is found in a range of natural settings, ranging from marine, to brackish and lacustrine, but is most commonly found in marine sediments forming below the sediment-water interface (e.g., Pauly, 1963; Steacy & Grant, 1974; Suess et al., 1982; Shearman & Smith, 1985; Jansen et al., 1987; Lu et al., 2012; Oehlerich et al., 2013; Scheller et al., 2021; Kennedy, 2022; Schultz et al., 2022). To date, the pre-requisites for natural ikaite precipitation over the more stable polymorphs are not fully understood.

This study examines ikaite to glendonite transformation, through geochemical and petrographic examination of transformed ikaite from the Isatkoak Lagoon, Utqiagvik (formerly called 'Barrow'), northern Alaska, and Holocene glendonites from the White Sea coast of the Kola Peninsula in Russia (Fig. 1). Through comparison with published data for other ikaites and glendonites, this study elucidates which palaeothermometric techniques may be used and how to reconstruct ikaite growth temperatures (key to paleoclimate studies that use glendonite as a paleotemperature proxy), and demonstrates the complexity of the chemical pre-requisites for ikaite growth in natural settings.

Regional geological setting

Utqiagvik lies some 15 km southwest of Point Barrow, the northernmost tip of Alaska (Fig. 1). Ice-wedge polygons cover almost the entire land surface with the landscape being underlain by continuous permafrost to depths in excess of 300 m (Ferrians, 1994). The average depth of seasonal thaw in the fine-grained surficial sediments is 0.4 m; with average yearly maximum (i.e., midsummer) air temperatures not exceeding 3°C . At Utqiagvik, the (modern) soil cover overlies the Pleistocene, transgressive Gubik Formation, which in turn overlies Cretaceous sandstone (Detterman et al., 1958; Brigham, 1983, 1985). The Walakpa gas field (containing methane gas and gas hydrates) is situated south of Utqiagvik, and the South Barrow gas fields underlie some of the coastal lagoons (Colett et al. 2011).

The Isatkoak Lagoon (c. 3 km long and 3 m deep) is situated within Utqiagvik (Fig. 1B; Pollen, 1987), and the lagoonal sediments comprise predominantly silt and fine gravelly sand (Brown, 1965; Hume, 1965; Green & Wharry, 2019). In 1000 AD, a flooding event built up a natural beach ridge that closed the connection between the original Isatkoak estuarine system and the sea. However, it is likely that this coastal bar has been breached multiple times since then. In 1978, a dam was constructed across Isatkoak Lagoon to create a new ponded water reservoir in the upper lagoon (Lynch et al., 2008), using material dredged from the lagoon itself, with some possibly coming from beach ridge sediments. The inland part of the lagoon has been progressively desalinated since the construction of the dam in order to provide a freshwater source for the Utqiagvik community (Pollen, 1987). Above the high-water mark, Ikaite crystals were discovered in an organic-rich clay bed along the east side of the causeway, and subsequently eroded and concentrated in the upper swash zone near the water's edge and less than 1 m above permafrost (Fig. 2) (Kennedy et al., 1987; Kennedy, 2022).

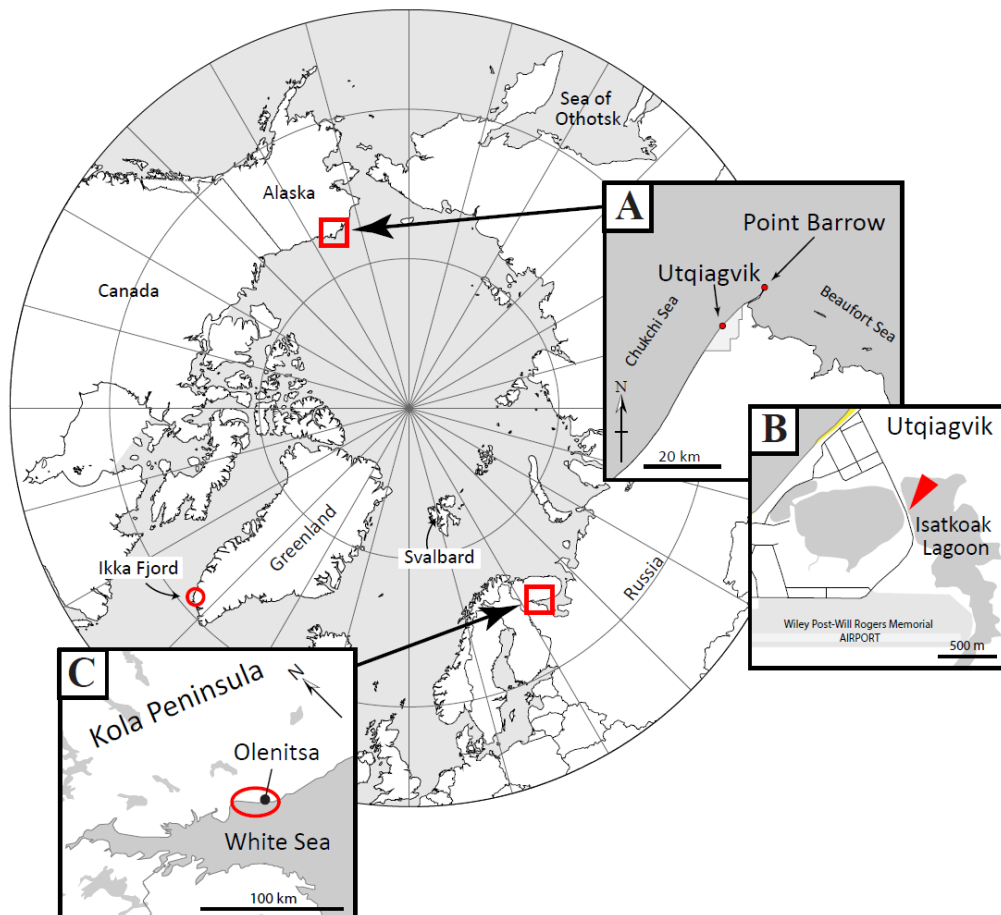


Figure 1. Map of the Arctic with localities discussed in the text indicated. (A) Map showing the northern tip of Alaska, with the city of Utqiagvik outlined in grey, and the Utqiagvik town centre marked by a red dot. (B) Detailed map of the Isatkoak Lagoon in Utqiagvik; the red pointer indicates where ikaite crystals were discovered in 1981 and recollected in 1983. (C) Detailed map of the White Sea region, red circle indicates where glendonites were collected (as analysed in this study and those of Vasileva et al., 2022 and Vickers et al., 2020).

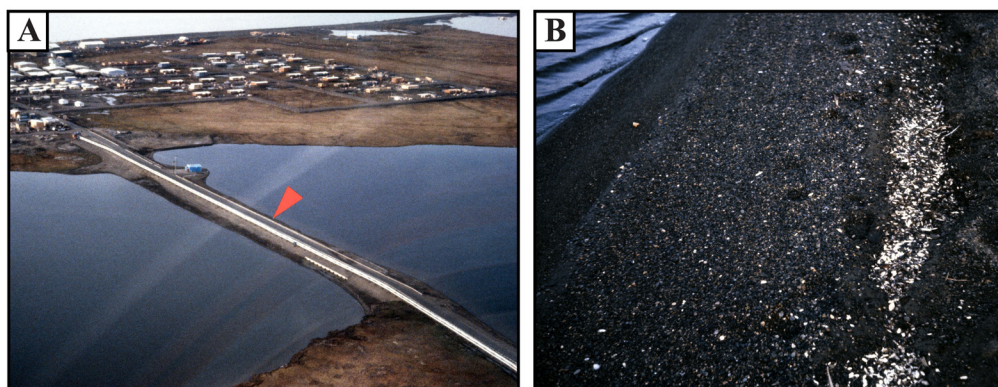


Figure 2. (A) Aerial view of Isatkoak Lagoon and causeway showing location (at pointer) of ikaite collection site. (B) White windrow of partially dehydrated ikaite crystals along the side of the causeway crossing the lagoon. Unaltered specimens were derived (eroded) from a black, organic-rich clay bed and subsequently concentrated in the wet pea gravel within the swash zone. Photos by G. L. Kennedy

White Sea

On the opposite side of the Arctic from Alaska, glendonites (calcite pseudomorphs after ikaite) are found in the Holocene tidal flats of Kandalaksha Bay, on the White Sea, between the Kola and Kanin peninsulas (Fig. 1). These marine–glaciomarine deposits comprise very fine-grained sands, silts and muds, with sporadic pebbles and boulders (e.g., Vasileva et al., 2022 and references therein). The glendonites are believed to be a maximum of c. 4000 years old, based on $^{230}\text{Th}/\text{U}$ dating of total dissolved glendonite (Vasileva et al., 2022).

Methods

A collection of hundreds of ikaite crystals (confirmed using XRD by Kennedy et al., 1987) from Isatkoak Lagoon was obtained in August of 1983, and subsequently kept frozen (currently at about -18°C) in home freezers (Kennedy, 2022). These were then transformed under ambient (room temperature) conditions (c. 21°C) and dried, prior to analysis. Glendonite samples from the White Sea were collected by digging 0.5–1 m into the tidal mud flats near the town of Olenitsa, in Kandalaksha Bay, and analysed for comparative purposes for this study, supplementing data from the recent publications of Vickers et al. (2020) and Vasileva et al. (2022).

Scanning Electron Microscopy with Energy Dispersive Spectroscopy (EDS) and Electron Backscatter Diffraction (EBSD)

Polished thin-sections of transformed Utqiagvik ikaite were carbon coated and analysed at Århus University with an Electron microprobe JEOLJXA-8600 at 15–20 kV, and a 1 nA beam. Elements analysed were Ca, Mg, Mn, Fe and Sr-bearing carbonates plus accessory minerals. A White Sea glendonite sample was prepared as a polished thin-section and analysed using a Hitachi SU5000 FE-SEM, equipped with Delmic Sparc CL system and Bruker EDS and HR EBSD system at the University of Oslo.

^{14}C Accelerator mass spectrometry (AMS)

Dating of the carbonates was undertaken on bulk pseudomorph by ^{14}C AMS at the Institut for Fysik og Astronomi, Århus Universitet using an HVE 1MV accelerator. The measured dates for marine carbonate samples are reported corrected for the ocean reservoir effect in order to be comparable to contemporaneous terrestrial material, by subtracting the ocean reservoir age (c. 400 years) from the conventional (measured) ^{14}C age. Calibrated ages in calendar years have been obtained from the marine model calibration curve (Marine13), using the Oxcal v4.1 programme with the probability method of Reimer et al. (2013). The marine model takes into account the smoothing in the world ocean of the sharper variations found in the atmospheric calibration curve. If not specifically stated otherwise, the local deviation (Delta-R) from the average world ocean model is assumed to be zero, corresponding to a standard reservoir age of 400 years.

The ^{14}C ages are reported in conventional radiocarbon years BP (before present = calendar year 1950) in accordance with international convention (Stuiver & Polach, 1977).

Inductively Coupled Plasma Optical Emission Spectrometry (ICP-OES)

Minor element analyses were undertaken on powdered, bulk-dried, transformed ikaite, now calcite, from Utqiagvik, Alaska, and the coast at Olenitsa, White Sea, Russia, using an Agilent 5110 VDV ICP-OES at the Camborne School of Mines, University of Exeter, following the method detailed in Ullmann et al. (2020). The minor element data are expressed as ratios to Ca and calibrated using certified single-element standards mixed to match the chemical composition of the analysed samples. Precision and accuracy of the analyses were measured and controlled by interspersing multiple measurements of international reference materials, JLS-1 and AK, and quality control solution (BCQ2).

Clumped and stable isotope analysis

The isotopic analysis was carried out on powdered bulk calcite from dried, transformed ikaite collected from Utqiagvik, Alaska, and on glendonites from Olenitsa, White Sea, Russia (Fig. 1). Clumped and stable isotope analysis was carried out at ETH Zürich using a ThermoFisher Scientific MAT253 mass spectrometer coupled to a Kiel IV carbonate preparation device, following the methods described in Müller et al. (2017). The Kiel IV device included a PoraPakQ trap kept at -40°C to eliminate potential organic contaminants. A maximum three replicates of each sample per session were measured, which consists generally of 24 samples of 100–120 µg interspersed with 5 replicates each of the carbonate standards ETH-1, ETH-2 and 10 replicates of ETH-3 (Bernasconi et al., 2018, 2021). The samples were analysed in LIDI mode with 400 seconds of integration of sample and reference gas. All calculations and corrections were done with the software Easotope (John & Bowen, 2016). The clumped isotope data are reported on the InterCarb carbon dioxide equilibration scale I-CDES (Bernasconi et al. 2021), and temperatures were calculated using the Anderson et al. (2021) calibration. Carbon and oxygen isotope compositions are reported in the conventional delta notation with respect to VPDB.

Results

Morphology of the ikaite and its pseudomorphs from Isatkoak Lagoon

The ikaite crystals and their pseudomorphs from Isatkoak Lagoon appear as single blades that have pseudo-mirror plane symmetry, with weakly imprinted prismatic faces in a pinacoid form (Fig. 3). The shape varies in the length to width ratio between the axis, with some showing more elongate forms (Fig. 3C). When allowed to dehydrate subaerially, the crystal form is typically retained, although there is significant internal volume loss as water is released from the structure. Thus, the resulting pseudomorphs are extremely fragile and susceptible to crumbling if handled after dehydration (Fig. 3B).

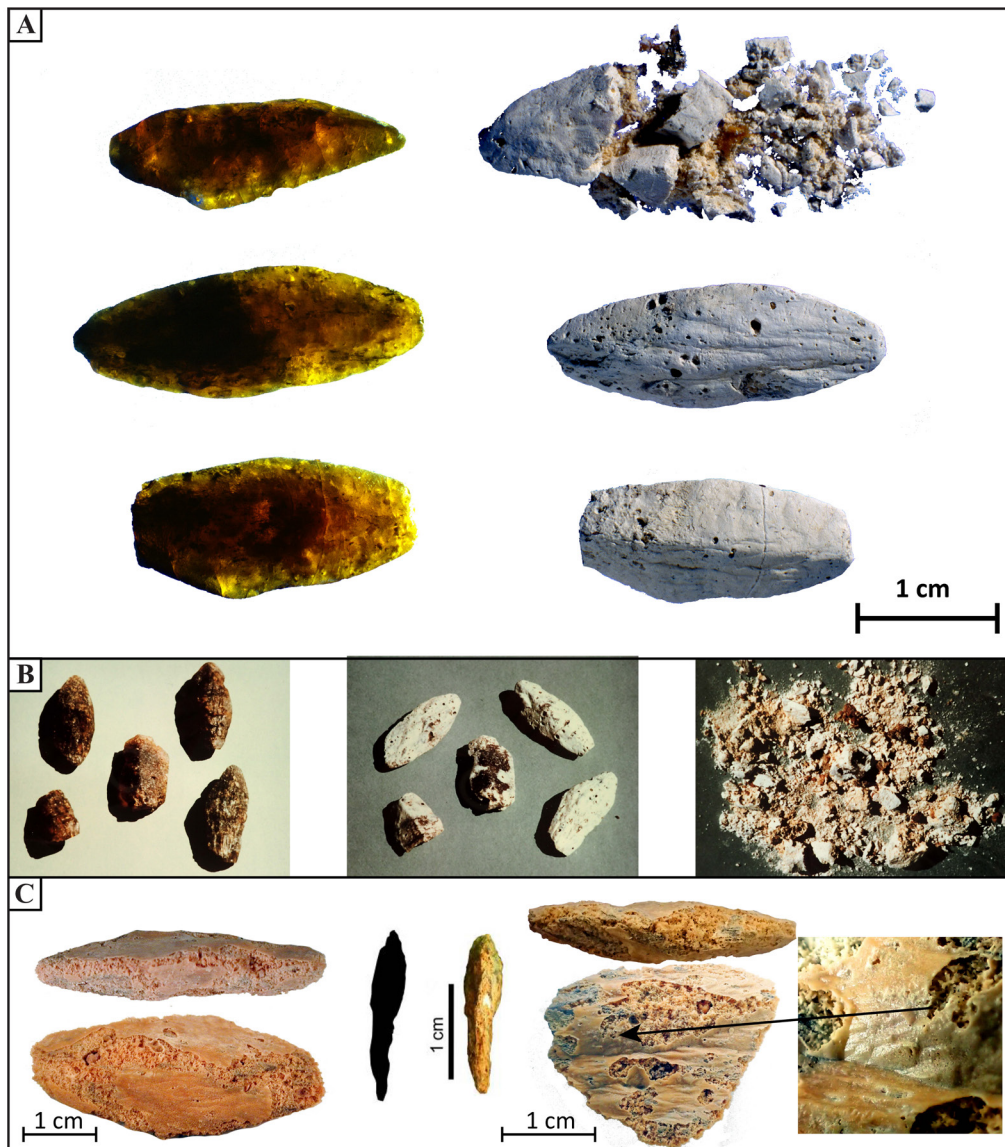


Figure 3. (A) Three specimens, 2–3 cm in length, of unaltered ikaite (left) recovered from the east side of the causeway crossing Isatkoak Lagoon (at pointer in Figs. 1B & 2A), and the same specimens (right) allowed to dehydrate to anhydrous CaCO_3 overnight. The specimen at the upper right crumbled to pieces when probed by the tip of a pencil the morning after it dehydrated. Photos by John DeLeon, Los Angeles. (B) Part of a series of photographs documenting the (untimed) dehydration process of ikaite to anhydrous CaCO_3 taken in 1987. Ikaite crystals were exposed to bright sunlight on a hot summer day. Left: Unaltered, at beginning of sequence. Centre: The same crystals partially dehydrated as indicated by surface colour change (white coating). Right: The same partially transformed ikaite after being broken apart to show the mixture of fragmented white and red-brown decay products. It is unknown if the hard brown parts of the middle crystal are ikaite or another product of the dehydration process. (C) Further examples of euhedral ikaite crystals transformed in air, at ambient temperatures (c. 20°C), clearly showing the outer 'crust' and porous centre. Left: a euhedral crystal pseudomorph viewed from one side and rotated 90° . Right: detail of the outer smooth "crust" of calcite, with the porous centre visible in the gaps in the crust.

SEM

The porous pseudomorphs have distinct structural components: a clear rim keeping the crystals from total collapse, and a highly porous centre made up of scattered larger and smaller calcite granules (Fig. 4A & B). The larger calcite granules are 1 to 3 mm in size with a rounded botryoidal morphology to the terminations of prismatic bodies and are zoned by colour (Fig. 4C) and porosity (Fig. 5C). The smaller granular crystals are 0.1 to 1 mm in size, 'dogtooth' scalenohedral type in shape, and elongated with sharp edges. The small crystals do not display any distinct zonation (Fig. 4).

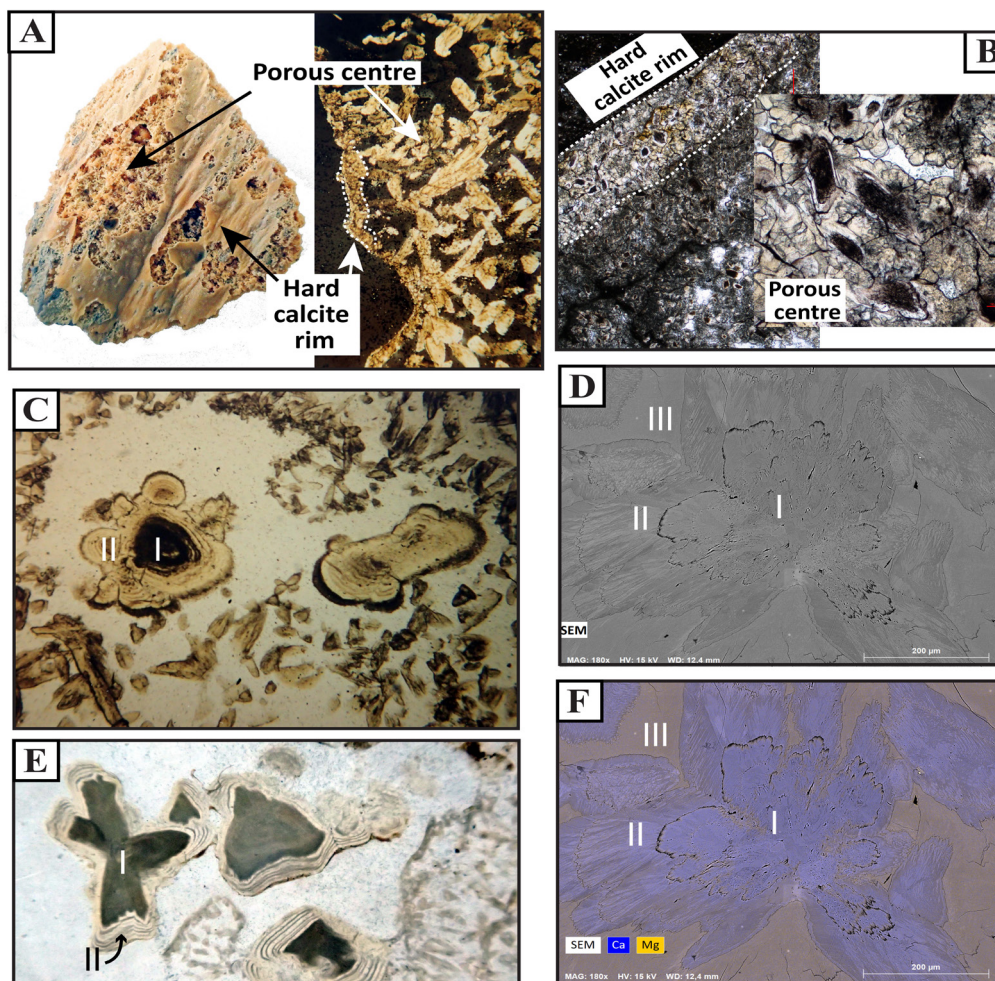


Figure 4. Microscopy images of Utqiagvik pseudomorphs and White Sea glendonites. (A) Utqiagvik pseudomorph showing outer calcite crust and porous centre and as it appears in thin-section. (B) White Sea glendonite under transmitted light showing the outer crust and porous centre; inset: detail of the 'guttalatic texture' at the centre of the sample. (C) & (E) Thin-section of Utqiagvik pseudomorph under transmitted and reflected light, respectively, showing larger granules with dark cores and colour-defined zoning. Type I and II calcite (as discussed in Vickers et al., 2018; 2020) labelled "I" and "II". (D) & (F) Detail of a zoned calcite bleb in White Sea glendonite thin-section. (D) shows the zoned calcite under secondary electrons; and (E) shows EDS maps for Ca and Mg overlain on D. Calcite Types I, II (ikaite-derived calcite) and III (late-stage sparry calcite) of Vickers et al. (2018) labelled.

SEM microprobe analysis shows the SrCO_3 , FeCO_3 and MnCO_3 contents to be low compared to CaCO_3 and MgCO_3 , with MgCO_3 negatively co-varying with CaCO_3 (Fig. 5). EDS maps show lowest Mg concentrations in the Type I calcite (Figs. 4C & 6B), with Mg-zoning only in Type II calcite. The zoning is therefore defined by chemical impurities (i.e., Mg) and porosity (Figs. 4–6).

AMS, clumped and stable isotopes, ICP-OES

Measured ^{14}C age, element ratios, clumped and stable isotope temperatures for the pseudomorphs analysed for this study are given in Table 1.

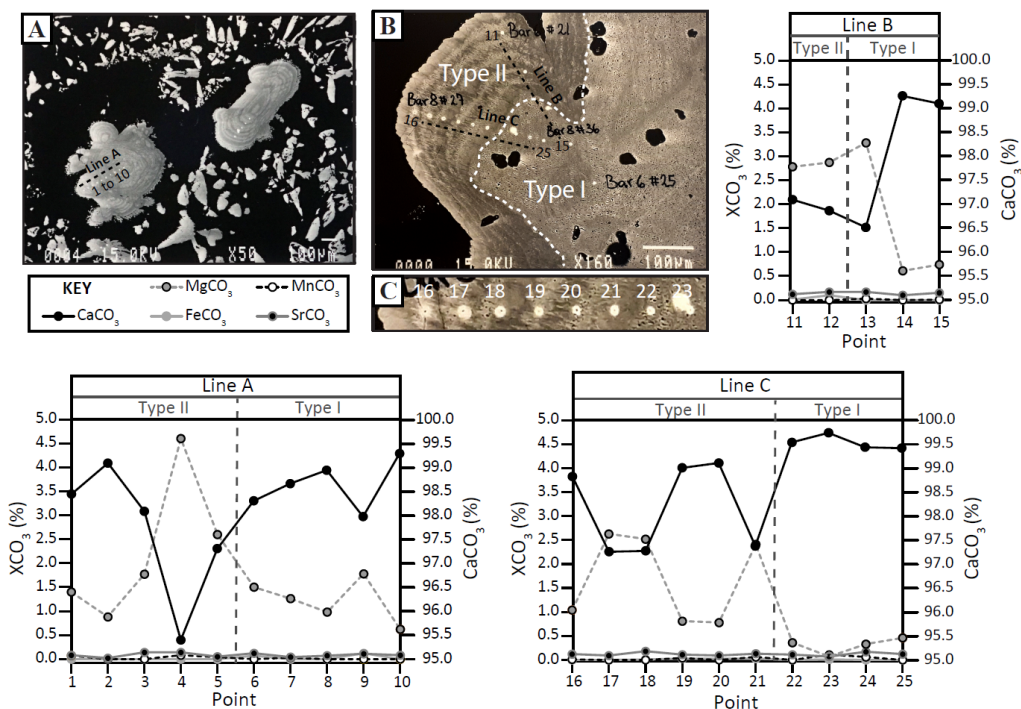


Figure 5. Microprobe elemental point data for Lines A, B and C and SEM images of the microprobe tracks. (A) SEM image of thin-section of Utqiaġvik pseudomorph under BSE. Dark and light zoning more distinct. Type I and II calcite (as discussed in Vickers et al., 2018; 2020) labelled “I” and “II”. Microprobe tracks (line A) burnt into the specimen. (B) Detail of microprobe tracks B and C under BSE. Calcite types I and II labelled. (C) Detail of Line C microprobe track. The zones can be seen to be defined by variation in porosity (light zones = more porous). Plotted microprobe measurements for elements Ca, Mg, Fe, Mn, Sr on thin-section of Utqiaġvik pseudomorph after ikaite for lines A, B and C as indicated in Fig. 4C, E & F.

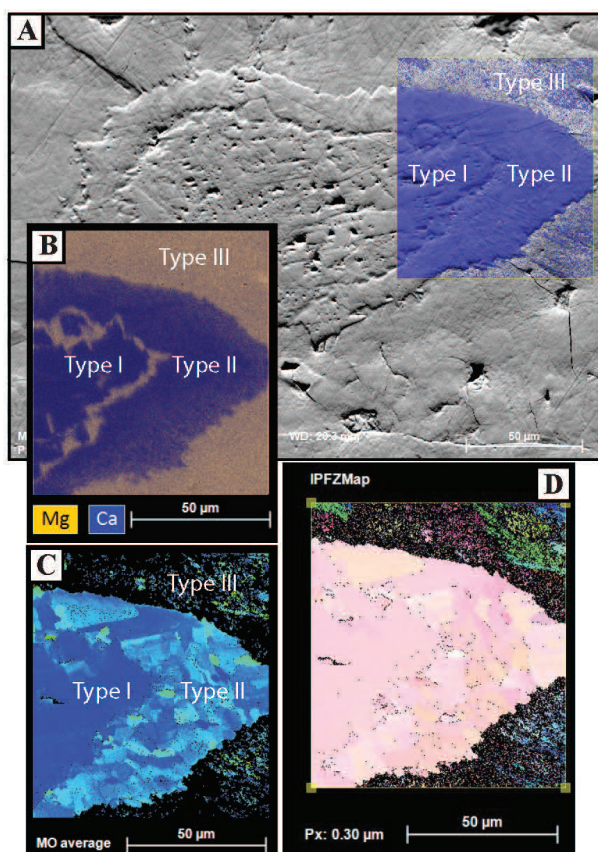


Figure 6. EBSD mapping zoned calcite in White Sea glendonite. (A) Secondary Electron (SE) image and phase map, showing the indexed pixels. (B) EDS element map showing high-Mg zones in otherwise low Mg ikaite-derived calcite (types I and II), compared to the homogenous, high-Mg sparry cement (type III). (C) Grain reference orientation deviation (misorientation, MO) map, which shows the misorientation between the orientation of every pixel in its respective position and the reference or mean orientation of the grain. Type I calcite is largely undistorted (blue), whereas Type II shows mild distortion (green-yellow), indicating it grew/formed differently from Type I; this may partially be due to the higher Mg-content of type II calcite. No strongly distorted grains (red) observed. (D) EBSD orientation map with inverse pole figure (IPF) colour-coding combined with image quality map.

Table 1. Summary of the geochemical results for the calcite pseudomorphs after ikaite from the Isatkoak Lagoon, Utqiaġvik, Alaska and the coast of Olenitsa in the White Sea, Russia. AMS – Accelerator Mass Spectrometry; pMC – percent modern carbon (modern defined as 1950). CI – Confidence Interval.

locality	sample type	AMS, U. Aarhus			Kiel Device, ETH Zürich									ICP-OES, U. Exeter					
		Corrected ¹⁴ C age	pMC	$\delta^{13}\text{C}$ AMS	Replica tes	$\delta^{13}\text{C}$ VPDB	$\delta^{18}\text{O}$ VPDB	$\delta^{18}\text{O}$ VSMO	Δ_{47} CDES	$\Delta_{47}\text{T}$ (°C)	-ve CI (°C)	+ve CI (°C)	$\delta^{18}\text{O}_{\text{fluid}}$ (‰ SMOW)	Mg/Ca (mmol /mol)	Sr/Ca (mmol /mol)	Mn/Ca (mmol /mol)	Fe/Ca (mmol /mol)	S/Ca (mmol /mol)	P/Ca (mmol /mol)
Utqiaġvik	pseudomorph after ikaite	1939 ± 28	78.56	-18	11	-19.40	-7.22	23.48	0.661	3.9	4.7	4.9	-9.3	1.64	0.872	0.013	1.239	3.21	0.26
			± 0.27			± 0.15	± 0.16												
White Sea	pseudomorph after ikaite	8559 ± 52	34.46	-19	12	-14.74	-1.23	29.65	0.664	2.3	-5.4	5.7	-3.7	50.63	1.599	0.129	0.54	1.2	11.5
			± 0.22			± 1.13	± 0.18												
White Sea	Shell	8835 ± 49	33.29	1															
			± 0.2																

Discussion

Morphology and petrography

The porous centres observed in the transformed ikaite crystals closely resemble the textures observed in certain Holocene glendonites from the White Sea in Russia (Vasileva et al., 2022). Because the transformation was in air, the pseudomorphs of the Utqiaġvik ikaites have not formed diagenetic calcite cements from the surrounding pore waters (unlike for more ancient glendonites e.g., Huggett et al., 2005; Frank et al., 2008; Qu et al., 2017; Morales et al., 2017; Vickers et al., 2018, 2020). Thus, the textures observed are features solely of the ikaite breakdown, and do not show secondary overgrowths from CaCO_3 derived from sources other than ikaite. The Utqiaġvik ikaite pseudomorphs show, for the larger grains, dark (organic-rich?) cores, with paler, zoned outer layers (Fig. 4). These morphologies have been described as “Type I” and “Type II” calcite phases, respectively, by Vickers et al. (2018) (e.g., as labelled in Fig. 4), and as a “guttalatic microtexture” by Scheller et al. (2021). Such dark cores are also observed in larger grains from the Holocene White Sea glendonites (Fig. 4B), 2 and also in the glendonites of the Palaeogene Fur Formation (Huggett et al., 2005; Vickers et al., 2020), although for other more thermally altered/poorly preserved glendonites the darkest-zoned part of the microfabric may be in the secondary calcite in zones around a lighter core (e.g., Frank et al., 2008; Morales et al., 2017; Qu et al., 2017). In transformed ikaite tufas from Mono Lake (California, USA), a similar zoned texture has been observed around pseudo-hexagonal or spherical calcite cores, although the cores are light rather than dark (Scheller et al., 2021). The Utqiaġvik pseudomorphs confirm that both phases (Types I and II) represent ikaite-derived calcite, and the EBSD data from the White Sea glendonites indicate that Type II (Mg-zoned) calcite grew on the Type I calcite, roughly following the same crystal alignment (Fig. 6). The alternation of high and low Mg zones (Figs. 4–6) is likely due to the fact that Mg is not as easily incorporated into the calcite structure (Vickers et al., 2022). During transformation, the Type I calcite therefore is believed to have formed rapidly, rejecting Mg, which went into the ikaite structural waters until it reached critical concentrations (e.g., at the transforming edge of the ikaite crystal) and was incorporated into the precipitating calcite (now Type II), forming a zone of high-Mg calcite (e.g., Figs. 4–6). This observation is in agreement with the coupled dissolution – reprecipitation mechanism for ikaite transformation as described by Tollefsen et al. (2020), and varies from that of Hiruta & Matsumoto (2022). These authors examined ikaite from Echigo Bank (Sea of Japan) and suggested that Mg was supplied from external pore waters surrounding Mg-free ikaite, and that it was the gradual contamination by Mg-rich water and the diluting effect of periodic ikaite breakdown that caused the observed Mg zoning. This cannot have occurred for the Utqiaġvik ikaites as they transformed in air (i.e., there were no external waters; the only water and elements came from the ikaite itself).

Environment of formation of the Utqiagvik ikaite

The minor element ratios for the transformed Utqiagvik ikaite are very close to that observed for transformed fully marine sedimentary ikaite (Fig. 7), despite the conditions in the Isatkoak Lagoon being chemically different (e.g., a brackish then subsequently desalinated environment). The Mg/Ca and S/Ca are much lower than those reported for both the glendonites and the concretions of the Fur Formation and White Sea carbonates, which may be partially due to the fact that these contain some diagenetic calcite phases as well as ikaite-derived calcite. The biotic carbonates measured from the White Sea have similar P/Ca, S/Ca, Mg/Ca, Mn/Ca and Fe/Ca ratios to the measured Utqiagvik transformed ikaite, although they contain higher Sr/Ca. The very low Mg/Ca ratios for the lagoonal Utqiagvik transformed ikaite and the fully marine transformed ikaites (Vickers et al., 2022) suggests that Mg did not play a significant role in stabilising ikaite in these settings; yet it may also simply be an artefact of Mg being less able to fit into the ikaite crystal structure than into calcite (e.g., as suggested by Vasileva et al., 2022 and Vickers et al., 2022).

The ^{14}C ages for this study (Table 1) are somewhat problematic to interpret, as the carbon sources for the ikaite are not fully known or quantified. It is important to note that they must reflect the (mixed) ages at which the carbon source(s) left the atmospheric system, and not the age of the crystallisation of the ikaite. This study returned a ^{14}C age for the White Sea glendonite sample of >8000 BP, in agreement with previous ^{14}C dates from Geptner et al. (1994), yet more than twice as old as that estimated by Vasileva et al. (2022) using U/Th dating (4100 ± 400 BP). The disparity between ^{14}C and U/Th dates indicates that much of the carbon in the White Sea glendonites had been out of the atmosphere for a long time before it was incorporated into the glendonites, either when the ikaite formed or when secondary cements formed after transformation. Without independent dating of the Utqiagvik ikaites, we cannot interpret the ^{14}C age.

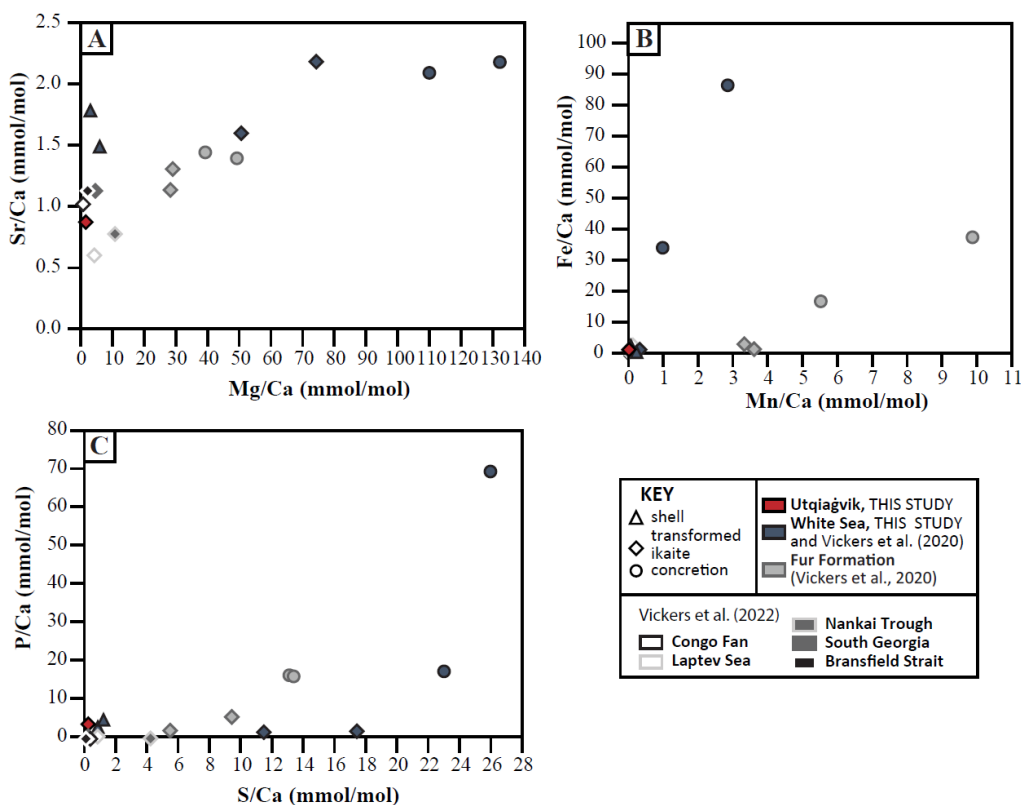


Figure 7. Element/Ca molar ratios for a Utqiagvik pseudomorph (this study) compared to published data for glendonites and coeval carbonates from Vickers et al. (2020).

The depleted $\delta^{13}\text{C}$ values for both measured carbonates (both Utqiagvik transformed ikaites and the White Sea pseudomorphs; Table 1 and Fig. 8) indicate that ocean-dissolved inorganic carbon (DIC) was not the sole source of carbon for these carbonates; either a large part of the carbon was derived from decaying organic matter (with average $\delta^{13}\text{C}$ values of c. -15 to -35‰; Campbell, 2006), or from methane ($\delta^{13}\text{C} < -40$ ‰; Campbell, 2006) (Fig. 8). There is an ongoing debate as to whether ikaite/glendonite requires anaerobic oxidation of methane to form (e.g., Greinert & Derkachev, 2004; Morales et al., 2017; Qu et al., 2017; Hiruta & Matsumoto et al., 2022), with other studies arguing that the breakdown of organic matter by sulphate-reducing bacteria generates the chemical conditions required to stabilise ikaite (e.g., high alkalinity and other chemical inhibitors of calcite) (Suess et al., 1982; Zabel & Schulz, 2001; Muramiya et al., 2022). The measured $\delta^{13}\text{C}$ values for both the Utqiagvik and the White Sea pseudomorphs are not within the range expected for methane seep carbonates (Fig. 8), and the dark brown colour observed in these and other marine sedimentary ikaites is believed to come from organic matter (e.g., Vickers et al., 2022 and references therein), supporting a strong contribution from organic matter to the $\delta^{13}\text{C}$ of the ikaites, and the hypothesis of organic matter breakdown by bacterial sulphate reduction creating the chemical conditions that stabilised ikaite over the other CaCO_3 polymorphs.

The ikaite clumped isotope temperatures from both the White Sea and the Utqiagvik pseudomorphs are within the range for known natural ikaite growth sites today (-2 to +7°C; Suess et al., 1982; Buchardt et al., 2001; Huggett et al., 2005; Hu et al., 2014; Zhou et al., 2015), and this is also within the range for the reconstructed clumped isotope temperatures of other transformed ikaites (e.g., Vickers et al., 2022) and for ancient glendonites (e.g., early Eocene Fur Formation ikaite-derived calcite, Vickers et al., 2020) (Fig 8). For the Utqiagvik pseudomorph this may initially appear surprising, since they transformed from ikaite to calcite at ambient room temperatures (c. 20°C), yet this reflects ikaite growth temperature rather than transformation temperature, supporting the hypothesised ikaite to calcite transformation being either quasi- solid state (i.e., as proposed in Vickers et al., 2022), or instantaneous dissolution-precipitation in the ikaite structural waters at the reaction interface (Tollefsen et al., 2020), such that equilibration with ambient conditions did not have time to occur (Guo, 2020).

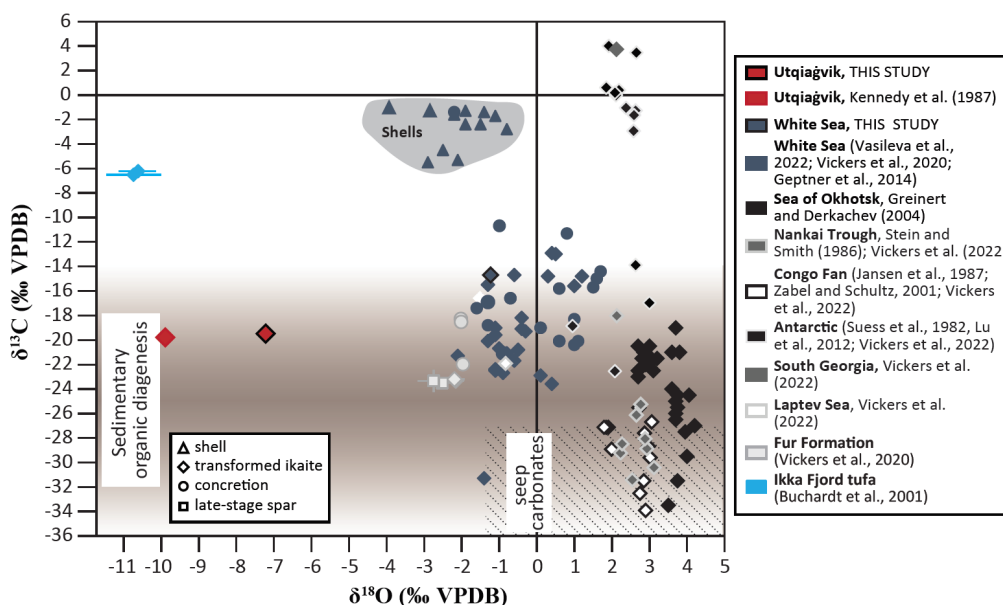


Figure 8. Stable isotope data for a Utqiagvik pseudomorph (this study) compared to published data for modern transformed ikaites, and selected glendonite data including glendonites from the Fur Formation and the White Sea, and other carbonates associated with those glendonites (references given in figure key). Hatched region indicates the expected field for methane seep carbonates (Campbell, 2006), with the range for sedimentary organic diagenesis indicated by the brown field (Campbell, 2006).

The measured $\delta^{18}\text{O}_{\text{carbonate}}$ of $<-7\text{‰}$ (this study and Kennedy et al., 1987) is much lighter than marine authigenic ikaite and glendonites; much closer to that of the Ikka Fjord tufa (c. -10‰ VPDB; Buchardt et al., 2001) (Fig. 9). Using the average clumped isotopic temperature for the Utqiagvik pseudomorphs to reconstruct the $\delta^{18}\text{O}$ of the fluid from which the carbonate precipitated, we get a value of around -9‰ SMOW (Fig. 9). Surface $\delta^{18}\text{O}_{\text{sw}}$ for the coast at Utqiagvik is expected to be around -2 to -3‰ (LeGrande & Schmidt, 2006), but the meteoric water is more depleted (e.g., Campbell, 2006). The reconstructed $\delta^{18}\text{O}_{\text{fluid}}$ of c. -9‰ for the Utqiagvik pseudomorphs (Fig. 9) is therefore consistent with a meteoric water source, suggesting that the ikaite grew authigenically in bottom sediments within a heavily meteorically-influenced system in keeping with the environment of the pre-dammed Isatkoak Lagoon, which may have been flooded sporadically by oceanic storm surges (cf., Lynch et al., 2008).

The environment of ikaite growth in the Isatkoak Lagoon thus differs from the more saline environments of the fully marine ikaites from the White Sea, Laptev Sea, Nankai Trough, Congo Fan and Antarctic shelf, reflected by heavier reconstructed $\delta^{18}\text{O}_{\text{fluid}}$ from the carbonates measured for clumped and stable isotopes (Table 1; Fig. 9). The relatively broad range in reconstructed $\delta^{18}\text{O}_{\text{fluid}}$ between the biotic and abiotic carbonates from the same sites likely arises due to the different ages of the carbonates (Vasileva et al., 2022). We note that the Fur Formation glendonites are from two different horizons (i.e., different ages) and several different phases of diagenetic growth were measured (ikaite-derived calcite, concretionary calcite and late-stage spar), likely accounting for the observed range in reconstructed $\delta^{18}\text{O}_{\text{fluid}}$ (Fig. 9).

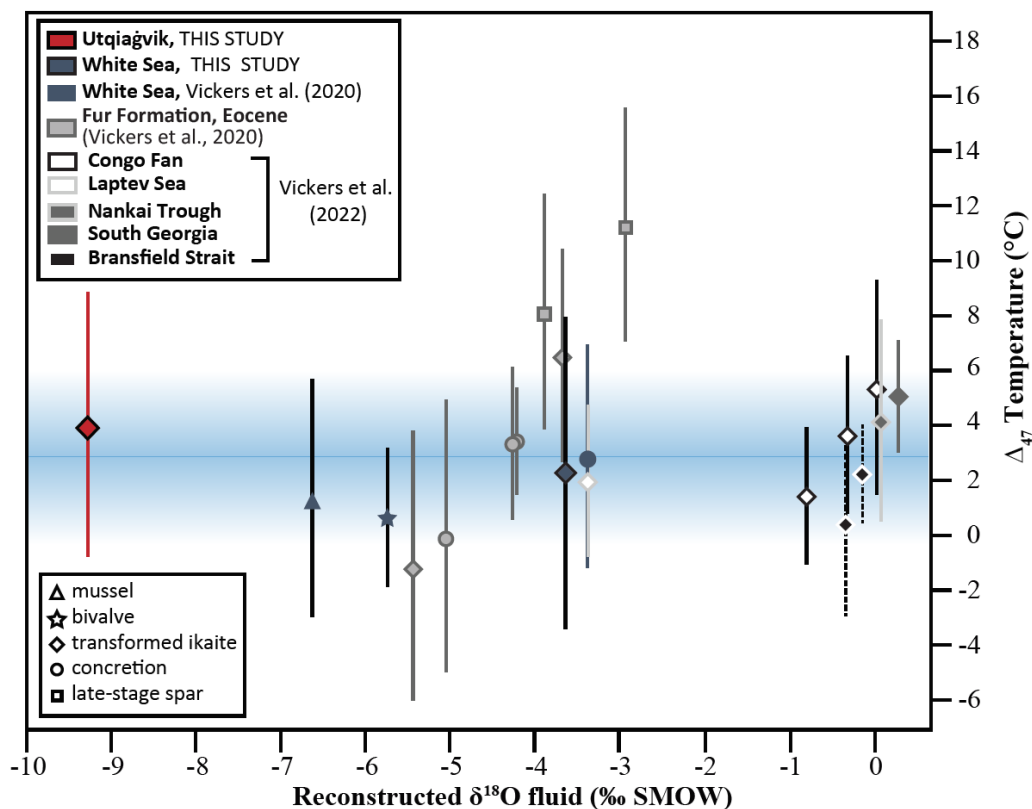


Figure 9. Clumped isotope temperatures for the Utqiagvik pseudomorph (i.e., ikaite transformed in air post-collection) compared to the White Sea and Fur Formation carbonates, plotted against reconstructed $\delta^{18}\text{O}_{\text{fluid}}$ (using the equation of Kim & O'Neil, 1997).

Conclusions

The Utqiagvik pseudomorphs after ikaite provide an example of transformed euhedral ikaite without subsequent diagenetic phases, indicating that the 'Type II' zoned calcite discussed in previous glendonite studies formed directly from ikaite CaCO_3 and does not represent a later diagenetic phase. Moreover, the zoning is observed both geochemically (by Mg/Ca variations), physically (by changes in porosity between various zones), and by colour (light/dark alternations). The results of combined clumped isotope and stable isotopic measurements suggest that the ikaite grew authigenically in bottom sediments within a fluvial/estuarine system, and used a predominantly organic carbon source, in accord with the proposed model for ikaite stabilisation by the bacterial breakdown of organic matter. The clumped isotope temperatures reconstructed for the ikaite pseudomorphs represent ikaite growth temperatures, indicating that the ikaite grew at a temperature of $c. 4 \pm 5^\circ\text{C}$.

Acknowledgements. G. L. Kennedy thanks USGS colleagues D. M. Hopkins and L. N. Marincovich for the opportunity to collaborate in their Alaskan field studies in 1981 and 1983. Funding was provided for this study by the European Commission, Horizon 2020 (ICECAP; grant no. 101024218) to M.L. Vickers, and from the Research Council of Norway through the Centres of Excellence funding scheme, project number 223272. The Research Council of Norway is acknowledged for support to the Goldschmidt Laboratory national infrastructure (project number 295894), and we thank Siri Simonsen for use and running of the SEM at the University of Oslo. Lastly, we thank the two anonymous reviewers for their constructive comments that have helped to improve the final manuscript. Thanks to Iñupiat Heritage Center and Army Corps of Engineers for informations, and to all Iñupiat inhabitants who has helped improving this paper.

References

- Anderson, N.T., Kelson, J.R., Kele, S., Daëron, M., Bonifacie, M., Horita, J., Mackey, T.J., John, C.M., Kluge, T., Petschnig, P. & Jost, A.B. 2021: A unified clumped isotope thermometer calibration ($0.5\text{--}1,100^\circ\text{C}$) using carbonate-based standardization. *Geophysical Research Letters* 48, e2020GL092069. <https://doi.org/10.1029/2020GL092069>
- Bernasconi, S.M., Müller, I.A., Bergmann, K.D., Breitenbach, S.F., Fernandez, A., Hodell, D.A., Jaggi, M., Meckler, A.N., Millan, I. & Ziegler, M. 2018: Reducing uncertainties in carbonate clumped isotope analysis through consistent carbonate-based standardization. *Geochemistry, Geophysics, Geosystems* 19, 2895–2914. <https://doi.org/10.1029/2017GC007385>
- Bernasconi, S.M., Daëron, M., Bergmann, K.D., Bonifacie, M., Meckler, A.N., Affek, H.P., Anderson, N., Bajnai, D., Barkan, E., Beverly, E. & Blamart, D. 2021: InterCarb: A community effort to improve interlaboratory standardization of the carbonate clumped isotope thermometer using carbonate standards. *Geochemistry, Geophysics, Geosystems* 22, e2020GC009588. <https://doi.org/10.1029/2020GC009588>
- Brigham, J.K. 1983: Correlation of late Cenozoic marine transgressions of the Arctic Coastal Plain with those in western Alaska and northeastern Russia. In *U.S. Geological Survey Polar Research Symposium – Abstracts with Program*. U.S. Geological Survey Circular 911, 47–52. <https://doi.org/10.3133/cir911>

- Brigham, J.K. 1985: *Marine stratigraphy and amino-acid geochronology of the Gubik Formation, western Arctic Coastal Plain, Alaska*. Ph.D. dissertation, University of Colorado, Boulder, 316 p.
- Brown, J. 1965: Radiocarbon Dating, Barrow, Alaska. *Arctic* 18, 37–48.
<https://doi.org/10.14430/arctic3448>
- Buchardt, B., Israelson, C., Seaman, P. & Stockmann, G. 2001: Ikaite tufa towers in Ikka Fjord, Southwest Greenland - their formation by mixing of seawater and alkaline springwater. *Journal of Sedimentary Research* 71, 1176–1189. <https://doi.org/10.1306/042800710176>
- Campbell, K.A. 2006: Hydrocarbon seep and hydrothermal vent paleoenvironments and paleontology: Past developments and future research directions. *Palaeogeography, Palaeoclimatology, Palaeoecology* 232, 362–407. <https://doi.org/10.1016/j.palaeo.2005.06.018>
- Collett, T.S., Lee, M.W., Agena, W.F., Miller, J.J., Lewis, K.A., Zyrianova, M.V., Boswell, R. & Inks, T.L. 2011: Permafrost-associated natural gas hydrate occurrences on the Alaska North Slope. *Marine and Petroleum Geology* 28, 279–294, <https://doi.org/10.1016/j.marpetgeo.2009.12.001>
- Detterman, R.L., Bowsher, A.L. & Dutro, J.T. 1958: Glaciation on the Arctic Slope of the Brooks Range, northern Alaska. *Arctic* 11, 43–61. <https://www.jstor.org/stable/40507180>
- Ferrians, O.J. 1994: Permafrost in Alaska. In Plafker, G. & Berg, H.C. (eds.): *The Geology of Alaska*, The Geology of North America Vol. G-1, pp. 845–854.
- Frank, T.D., Thomas, S.G. & Fielding, C.R. 2008: On using carbon and oxygen isotope data from glendonites as paleoenvironmental proxies: a case study from the Permian system of eastern Australia. *Journal of Sedimentary Research* 78, 713–723. <https://doi.org/10.2110/jsr.2008.081>
- Geptner, A.R., Pokrovsky, B.G., Sadchikova, T.A., Sulerzhitsky, L.D. & Chernyakhovsky, A. G. 1994: Local carbonatization of sediments of the White Sea (concept of microbiological formation). *Litol. Polezn. Iskop.* 5, 3–22.
- Green, R.J. & Wharry, S. 2019: Barrow Alaska Coastal Erosion Feasibility Study, Appendix F: Geotechnical, *US Army Corps of Engineers, Alaska District*, pp. 1–40.
- Greinert, J. & Derkachev, A. 2004: Glendonites and methane-derived Mg-calcites in the Sea of Okhotsk, Eastern Siberia: implications of a venting-related ikaite/glendonite formation. *Marine Geology* 204, 129–144. [https://doi.org/10.1016/S0025-3227\(03\)00354-2](https://doi.org/10.1016/S0025-3227(03)00354-2)
- Guo, W. 2020: Kinetic clumped isotope fractionation in the DIC–H₂O–CO₂ system: patterns, controls, and implications. *Geochimica et Cosmochimica Acta* 268, 230–257.
<https://doi.org/10.1016/j.gca.2019.07.055>
- Hiruta, A. & Matsumoto, R. 2022: Geochemical comparison of ikaite and methane-derived authigenic carbonates recovered from Echigo Bank in the Sea of Japan. *Marine Geology* 443, 106672.
<https://doi.org/10.1016/j.margeo.2021.106672>
- Hu, Y.B., Wolf-Gladrow, D.A., Dieckmann, G.S., Völker, C. & Nehrke, G. 2014: A laboratory study of ikaite (CaCO₃·6H₂O) precipitation as a function of pH, salinity, temperature and phosphate concentration. *Marine Chemistry* 162, 10–18. <https://doi.org/10.1016/j.marchem.2014.02.003>

- Huggett, J.M., Schultz, B.P., Shearman, D.J. & Smith, A.J. 2005: The petrology of ikaite pseudomorphs and their diagenesis. *Proceedings of the Geologists' Association* 116, 207–220.
[https://doi.org/10.1016/S0016-7878\(05\)80042-2](https://doi.org/10.1016/S0016-7878(05)80042-2)
- Hume, J.D. 1965: Sea-level changes during the last 2000 years at Point Barrow, Alaska. *Science* 150, 1165–1166. <https://doi.org/10.1126/science.150.3700.1165>
- Jansen, J., Woensdregt, C., Kooistra, M. & Van Der Gaast, S. 1987: Ikaite pseudomorphs in the Congo deep-sea fan: an intermediate between calcite and porous calcite. *Geology* 15, 245–248.
[https://doi.org/10.1130/0091-7613\(1987\)15<245:IPITZD>2.0.CO;2](https://doi.org/10.1130/0091-7613(1987)15<245:IPITZD>2.0.CO;2)
- John, C.M. & Bowen, D. 2016: Community software for challenging isotope analysis: First applications of 'Easotope' to clumped isotopes. *Rapid Communications in Mass Spectrometry* 30, 2285–2300.
<https://doi.org/10.1002/rcm.7720>
- Kemper, E. 1987: *Das Klima der Kreide-Zeit*. Geologisches Jahrbuch, Hannover, 5–185.
- Kennedy, G.L. 2022: Glendonites: Enigmatic mineral pseudomorphs and their ephemeral precursor. *Rocks & Minerals* 97, 496–508. <https://doi.org/10.1080/00357529.2022.2087146>
- Kennedy, G.L., Hopkins, D.M. & Pickthorn, W.J. 1987: Ikaite, the glendonite precursor, in estuarine sediments at Barrow, Arctic Alaska. *Annual Meeting Abstract Program 9, Geological Society of America*, pp. 725.
- Kim, S.T. & O'Neil, J.R. 1997: Equilibrium and nonequilibrium oxygen isotope effects in synthetic carbonates. *Geochimica et Cosmochimica Acta* 61, 3461–3475.
[https://doi.org/10.1016/S0016-7037\(97\)00169-5](https://doi.org/10.1016/S0016-7037(97)00169-5)
- LeGrande, A.N. & Schmidt, G.A. 2006: Global gridded data set of the oxygen isotopic composition in seawater. *Geophysical Research Letters* 33, L12604. <https://doi.org/10.1029/2006GL026011>
- Lu, Z., Rickaby, R.E., Kennedy, H.A., Kennedy, P., Pancost, R.D., Shaw, S., Lennie, A., Wellner, J. & Anderson, J.B. 2012: An ikaite record of late Holocene climate at the Antarctic Peninsula. *Earth and Planetary Science Letters* 325, 108–115. <https://doi.org/10.1016/j.epsl.2012.01.036>
- Lynch, A.H., Lestak, L.R., Uotila, P., Cassano, E.N. & Xie, L. 2008: A factorial analysis of storm surge flooding in Barrow, Alaska. *Monthly Weather Review* 136, 898–912. <https://doi.org/10.1175/2007MWR2121.1>
- Morales, C., Rogov, M., Wierzbowski, H., Ershova, V., Suan, G., Adatte, T., Föllmi, K.B., Tegelaar, E., Reichart, G.-J., de Lange, G.J., Middleburg, J.J. & van de Schootbrugge, B. 2017: Glendonites track methane seepage in Mesozoic polar seas. *Geology* 45, 503–506. <https://doi.org/10.1130/G38967.1>
- Müller, I.A., Fernandez, A., Radke, J., Van Dijk, J., Bowen, D., Schwieters, J. & Bernasconi, S.M. 2017: Carbonate clumped isotope analyses with the long-integration dual-inlet (LIDI) workflow: Scratching at the lower sample weight boundaries. *Rapid Communications in Mass Spectrometry* 31, 1057–1066.
<https://doi.org/10.1002/rcm.7878>
- Muramiya, Y., Yoshida, H., Minami, M., Mikami, T., Kobayashi, T., Sekiuchi, K. & Katsuta, N. 2022: Glendonite concretion formation due to dead organism decomposition. *Sedimentary Geology* 429, 106075. <https://doi.org/10.1016/j.sedgeo.2021.106075>

Oehlerich, M., Mayr, C.C., Griesshaber, E., Lücke, A., Oeckler, O.M., Ohlendorf, C., Schmahl, W.W. & Zolitschka, B. 2013: Ikaite precipitation in a lacustrine environment – implications for palaeoclimatic studies using carbonates from Laguna Potrok Aike (Patagonia, Argentina). *Quaternary Science Review* 71, 46–53. <https://doi.org/10.1016/j.quascirev.2012.05.024>

Pauly, H. 1963: "Ikaite", a new mineral from Greenland. *Arctic* 16, 263–264. <https://doi.org/10.14430/arctic3545>

Pollen, M.R. 1987: Water conservation and management in Barrow, Alaska. *Journal of the American Water Works Association* 79, 26–34. <https://doi.org/10.1002/j.1551-8833.1987.tb02811.x>

Purgstaller, B., Dietzel, M., Baldermann, A. & Mavromatis, V. 2017: Control of temperature and aqueous Mg²⁺/Ca²⁺ ratio on the (trans-) formation of ikaite. *Geochimica et Cosmochimica Acta* 217, 128–143. <https://doi.org/10.1016/j.gca.2017.08.016>

Qu, Y., Teichert, B., Birgel, D., Goedert, J. & Peckmann, J. 2017: The prominent role of bacterial sulfate reduction in the formation of glendonite: a case study from Paleogene marine strata of western Washington State. *Facies* 63, 10. <https://doi.org/10.1007/s10347-017-0492-1>

Reimer, P.J., Bard, E., Bayliss, A., Beck, J.W., Blackwell, P.G., Ramsey, C.B., Buck, C.E., Cheng, H., Edwards, R.L., Friedrich, M. & Grootes, P.M. 2013: IntCal13 and Marine13 radiocarbon age calibration curves 0–50,000 years cal BP. *Radiocarbon* 55, 1869–1887. https://doi.org/10.2458/azu_js_rc.55.16947

Rogov, M.A., Ershova, V., Vereshchagin, O., Vasileva, K., Mikhailova, K. & Krylov, A. 2021: Database of global glendonite and ikaite records throughout the Phanerozoic. *Earth System Science Data* 13, 343–356. <https://doi.org/10.5194/essd-13-343-2021>

Scheller, E.L., Grotzinger, J. & Ingalls, M. 2021: Guttulatic calcite: A carbonate microtexture that reveals frigid formation conditions. *Geology* 50, 48–53. <https://doi.org/10.1130/G49312.1>

Schultz, B.P., Thibault, N. & Huggett, J.M. 2022: The minerals ikaite and its pseudomorph glendonite: Historical perspective and legacies of Douglas Shearman and Alec K. Smith. *Proceedings of the Geologists' Association* 133, 176–192. <https://doi.org/10.1016/j.pgeola.2022.02.003>

Shearman, D.J. & Smith, A.J. 1985: Ikaite, the parent mineral of jarrowite-type pseudomorphs. *Proceedings of the Geologists' Association* 96, 305–314. [https://doi.org/10.1016/S0016-7878\(85\)80019-5](https://doi.org/10.1016/S0016-7878(85)80019-5)

Stacey, H.R. & Grant, D.R. 1974: Tidal muds reveal mineral curiosity. *Canadian Geographical Journal* 88, 36–38.

Stockmann, G., Tollefsen, E., Skelton, A., Brüchert, V., Balic-Zunic, T., Langhof, J., Skogby, H. & Karlsson, A. 2018: Control of a calcite inhibitor (phosphate) and temperature on ikaite precipitation in Ikka Fjord, southwest Greenland. *Applied Geochemistry* 89, 11–22. <https://doi.org/10.1016/j.apgeochem.2017.11.005>

Stuiver, M. & Polach, H.A. 1977: Discussion of reporting C¹⁴ data. *Radiocarbon* 19, 355. <https://doi.org/10.1017/S0033822200003672>

Suess, E., Balzer, W., Hesse, K.-F., Muller, P. J., Ungerer, C. A. & Wefer, G. 1982: Calcium carbonate hexahydrate from organic-rich sediments of the Antarctic shelf: Precursors of glendonites. *Science* 216, 1128–1131. <https://doi.org/10.1126/science.216.4550.1128>

Tollefsen, E., Balic-Zunic, T., Morth, C.-M., Bruchert, V., Lee, C.C. & Skelton, A. 2020: Ikaite nucleation at 35 degrees C challenges the use of glendonite as a paleotemperature indicator. *Science Reporter* 10, 8141. <https://doi.org/10.1038/s41598-020-64751-5>

Ullmann, C.V., Boyle, R., Duarte, L., Hesselbo, S., Kasemann, S., Klein, T., Lenton, T., Piazza, V. & Aberhan, M. 2020: Warm afterglow from the Toarcian Oceanic Anoxic Event drives the success of deep-adapted brachiopods. *Scientific Reports* 10, 1–11. <https://doi.org/10.1038/s41598-020-63487-6>

Vasileva, K., Zaretskaya, N., Ershova, V., Rogov, M., Stockli, L.D., Stockli, D., Khaitov, V., Maximov, F., Chernyshova, I., Soloshenko, N. & Frishman, N. 2022: New model for seasonal ikaite precipitation: Evidence from White Sea glendonites. *Marine Geology* 449, 106820. <https://doi.org/10.1016/j.margeo.2022.106820>

Vickers, M., Watkinson, M., Price, G.D., Jerrett, R., 2018. An improved model for the ikaite-glendonite transformation: evidence from the Lower Cretaceous of Spitsbergen, Svalbard. *Norwegian Journal of Geology* 98, 1–15. <https://dx.doi.org/10.17850/njg98-1-01>

Vickers, M.L., Lengger, S.K., Bernasconi, S.M., Thibault, N., Schultz, B.P., Fernandez, A., Ullmann, C.V., McCormack, P., Bjerrum, C.J. & Rasmussen, J.A. 2020: Cold spells in the Nordic Seas during the early Eocene Greenhouse. *Nature Communications* 11, 1–12. <https://doi.org/10.1038/s41467-020-18558-7>

Vickers, M.L., Vickers, M., Rickaby, R.E., Wu, H., Bernasconi, S.M., Ullmann, C.V., Bohrmann, G., Spielhagen, R.F., Kassens, H., Schultz, B.P. & Alwmark, C. 2022: The ikaite to calcite transformation: implications for palaeoclimate studies. *Geochimica et Cosmochimica Acta* 334, 201–216. <https://doi.org/10.1016/j.gca.2022.08.001>

Zabel, M. & Schulz, H.D. 2001: Importance of submarine landslides for non-steady state conditions in pore water systems—lower Zaire (Congo) deep-sea fan. *Marine Geology* 176, 87–99. [https://doi.org/10.1016/S0025-3227\(01\)00164-5](https://doi.org/10.1016/S0025-3227(01)00164-5)

Zhou, X., Lu, Z., Rickaby, R.E.M., Domack, E.W., Wellner, J.S. & Kennedy, H.A. 2015: Ikaite abundance controlled by porewater phosphorus level: potential links to dust and productivity. *The Journal of Geology* 123, 269–281. <https://doi.org/10.1086/681918>